

Experiments on Adaptive Nonlinear Model Predictive Control of a Pendulum

Fabian Schnelle and Peter Eberhard

Institute of Engineering and Computational Mechanics, University of Stuttgart, Germany

Summary. This work presents the simulative and experimental application of an adaptive nonlinear model predictive control scheme on a pendulum. The control objective is both a disturbance rejection and an accurate trajectory tracking in the presence of uncertainties, which is realized by a cascade control structure consisting of a position control and an adaptive model predictive controller. Uncertainties such as external disturbances or unmodeled dynamics are considered in the adaptive MPC design by estimating the dynamics of the prediction model with an Unscented Kalman Filter online and based on that, adapting the optimization problem in each time step. In order to investigate the effect of uncertainties on the performance of the proposed control structure, simulation results provided by a fuzzy-arithmetical analysis are compared with experimental results.

Introduction

Model-based approaches for the control of mechanical systems typically lead to satisfying results. As in the presence of model uncertainties or external disturbances some of these approaches reach their limits, adaptive control schemes are needed in order to incorporate their effect in the control design. Adaptive control deals with the correct adjustment of control parameters online [1], where also in the field of robotics and mechanical systems many approaches exist [13, 9]. Model predictive control (MPC) is an optimization-based control technique of increasing importance usable for widespread industrial applications [7, 8]. Based on the prediction of the future dynamical behaviour of the plant, an optimal input sequence is found by solving an optimization problem over a certain horizon. After implementing the first input of the sequence and shifting the prediction horizon, the optimal control problem is repeated. Due to its capability of forecasting the future dynamical behaviour and consideration of constraints like mechanical limitations, MPC is very suitable for tracking control purposes occurring in linear and nonlinear systems. This paper presents an adaptive MPC design, where the prediction model is updated online by a parameter estimation which is performed by an Unscented Kalman Filter (UKF). This leads to an adaptation of the optimization problem in each time step and, thus, to a better prediction and an improved control action. The proposed control scheme is applied to a pendulum moving in three-dimensional space, for which both simulative and experimental investigations are made. The investigations include both the design for the undisturbed system and a disturbed system, where two types of uncertainties are implemented in order to verify the functionality of the presented control structures. Simulation results provided by a fuzzy-arithmetical analysis are compared with experimental results.

Experimental Setup and Mechanical Model of the Pendulum

Experimental Setup

The pendulum, which is depicted in Figure 1, consists of a sphere at the end of a thin rod. The rod is mounted on gimbals on a cross table consisting of three toothed belt axes. The third axis (x-direction) is mounted onto the other two axes (y-direction) which are coupled with a shared motor and synchronised using a connecting shaft. Both carts are driven by DC motors which enable the pendulum performing three-dimensional oscillations. The motors operate in current control mode and receive their signals via servo amplifiers which are coupled with the real-time system dSPACE. It should also be noted that both cart positions and both Cardan angles are measured by incremental encoders. Components of the experimental infrastructure are shown in Figure 2.

Mechanical Model

The schematic model of the pendulum is depicted in Figure 3. The orientation of the thin rod (mass m_r , inertia I_r , length L_r) with the fixed sphere (mass m_s , inertia I_s) can be described by the Cardan angles α and β . The cart positions are denoted by x_c , respectively y_c , and are driven by the motor torques T_1 and T_2 . As the motors operate in current control mode, the current signals I_1 and I_2 are calculated from the motor torques via the proportional dependency $T_i = k_M I_i$. Following the principles of Newton and Euler and d'Alembert the nonlinear equations of motion of this multibody system can be derived

$$M(\mathbf{q})\ddot{\mathbf{q}} + \mathbf{k}(\mathbf{q}, \dot{\mathbf{q}}) = \mathbf{g}(\mathbf{q}, \dot{\mathbf{q}}) + \mathbf{B}\bar{\mathbf{u}} \quad (1)$$

with the generalized coordinates $\mathbf{q} = [x_c \ y_c \ \alpha \ \beta]^T$ and the inputs $\bar{\mathbf{u}} = [T_1 \ T_2]^T$. The symmetric positive definite matrix M is known as the mass matrix. The vector \mathbf{k} summarizes the Coriolis, centrifugal and gyroscopic forces, whereby the generalized applied forces are expressed by the vector \mathbf{g} . The matrix B distributes the control inputs $\bar{\mathbf{u}}$ onto the directions of the generalized coordinates. It should be noted that both elastic deformations of the bodies and friction in the toothed belt axes are neglected in this model. The most important material parameters are summarized in Table 1.

Adaptive Controller Design

The controller design aims at trajectory tracking of the center of gravity of the sphere position $\mathbf{r}(\mathbf{q})$. A control law on the basis of (1) can not be established as the toothed belt axes have non-negligible static and dynamical frictional torques

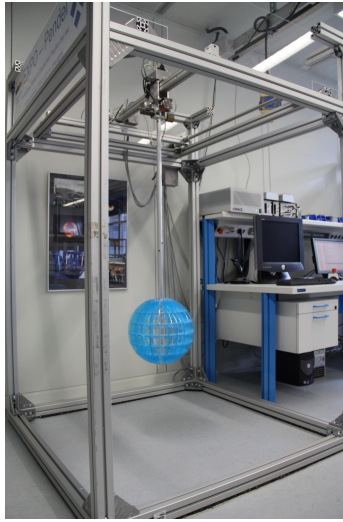


Figure 1: Experimental setup of the pendulum.



Figure 2: dSPACE autobox (top left), servo amplifiers (top right), Cardan joint and encoders (bottom left), DC motor (bottom right).

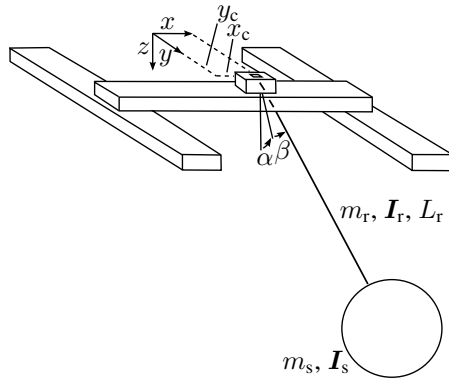


Figure 3: Schematic model of the pendulum.

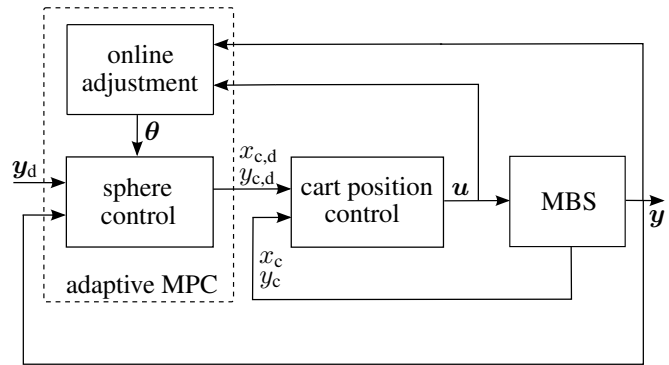


Figure 4: Cascade control structure with adaptive MPC.

whose mathematical descriptions are not trivial. For instance, the carts do not move without power supply, although the pendulum is performing oscillations. Furthermore, there exist unmodeled bodies like additional masses and cables causing unknown dynamical effects. Beside these mentioned limitations, the effect of external disturbances on the performance of the controller should be as small as possible which leads to the choice of an adaptive control structure. Control approaches for the pendulum in the presence of no uncertainties can be found in [12, 10].

Cascade Control

An effective way to compensate these frictional effects and the uncertainties in the model is the use of a cascade control structure which is depicted in Figure 4. The inner loop is controlled by a fast PD controller to guarantee the accordance of the target and the actual cart position. The control target of the outer loop is the robust trajectory tracking of the sphere position, wherefore an adaptive MPC is designed. As the original states x_c, y_c are now control inputs, a new dynamical model has to be derived which is the basis for the controller design of the outer loop. For this purpose (1) is partitioned and rewritten with the appropriate dependencies

$$\begin{bmatrix} M_{11} & M_{12}(q_2) \\ M_{12}^T(q_2) & M_{22}(q_2) \end{bmatrix} \begin{bmatrix} \ddot{q}_1 \\ \ddot{q}_2 \end{bmatrix} + \begin{bmatrix} k_1(q_2, \dot{q}_2) \\ k_2(q_2, \dot{q}_2) \end{bmatrix} = \begin{bmatrix} g_1(q_2, \dot{q}_2) \\ g_2(q_2, \dot{q}_2) \end{bmatrix} + \begin{bmatrix} B_1 \\ \mathbf{0} \end{bmatrix} \bar{u} \quad (2)$$

with the partitioned generalized coordinates $q_1 = [x_c \ y_c]^T$ and $q_2 = [\alpha \ \beta]^T$. Defining the new input $u := q_1$ the lower part of (2) denotes the reduced equations of motion and can be rewritten as

$$M_{22}(q_2)\ddot{q}_2 + k_2(q_2, \dot{q}_2) = g_2(q_2, \dot{q}_2) - M_{12}^T(q_2)\ddot{u} \quad (3)$$

Table 1: Some material parameters of the pendulum.

| parameter | mass m_r | inertia $I_{r,x}$ | length L_r | mass m_s | inertia $I_{s,x,y,z}$ |
|-----------|------------|-------------------------|--------------|------------|------------------------|
| value | 1.1 kg | 0.0525 kgm ² | 1.12 m | 4.05 kg | 0.095 kgm ² |

which describes the dynamics from the cart accelerations to the Cardan angles. It is here appropriate to linearize (3) and the sphere position $r(\mathbf{q})$ with respect to their lower equilibrium point $\mathbf{q}_s = [0 \ 0 \ 0 \ 0]^T$ and $\mathbf{u}_s = [0 \ 0]^T$ as the sphere is desired to oscillate around its equilibrium. After Jacobian linearization and time discretization the obtained equations can be stated in discrete state space form

$$\mathbf{x}_{k+1} = \mathbf{A}\mathbf{x}_k + \mathbf{B}\mathbf{u}_k, \quad (4)$$

$$\mathbf{y}_k = \mathbf{C}\mathbf{x}_k + \mathbf{D}\mathbf{u}_k \quad (5)$$

with the input vector $\mathbf{u} = [x_c \ y_c]^T$ and the output vector \mathbf{y} representing the sphere position. It is worth to mention that the state vector \mathbf{x} contains non-physical variables. The reason for this is that (3) is influenced by the acceleration $\ddot{\mathbf{u}}$, whereas (4) and (5) are supposed to be controlled by the position \mathbf{u} . Therefore, the system has to be stated in controllable canonical form and consequently loses the physical meaning of its states. It should also be noted that the feedthrough term \mathbf{D} is non-zero due to the fact that the sphere position is directly influenced by the cart positions. The dynamics of the linearized equations of motion is discretized as the MPC is typically based on a time-discrete state space model given by (4) and (5).

Adaptive Linear Model Predictive Control Algorithm

Before establishing the adaptive MPC scheme, the idea behind MPC is very briefly introduced. Based on the prediction of the future dynamical behaviour of the plant, an optimal input sequence is found by solving an optimization problem over a certain horizon. After implementing the first input of the sequence and shifting the prediction horizon, the optimal control problem is solved again, see [7]. The optimal control problem is given by minimizing the quadratic cost function

$$J = \sum_{i=k}^{k+P-1} \|\mathbf{y}_i - \mathbf{y}_{d,i}\|_Q^2 + \|\Delta\mathbf{u}_i\|_R^2 \quad (6)$$

over the input trajectory $\Delta\mathbf{U} = [\Delta\mathbf{u}_k^T \ \cdots \ \Delta\mathbf{u}_{k+M-1}^T]^T$ considering the system dynamics (4) and (5) and constraints on the input \mathbf{u} . The prediction horizon P defines the number of future time steps over which the dynamics is predicted, whereas the control horizon M defines the dimension of the optimization variable \mathbf{U} . The weighting matrices \mathbf{Q} and \mathbf{R} are tuning parameters in order to define the control objective. The accuracy can be adjusted by \mathbf{Q} penalizing the deviation from the reference trajectory \mathbf{y}_d , whereas the aggressivity of the controller can be tuned by \mathbf{R} . In order to solve the optimal control problem $\min_{\Delta\mathbf{U}} J$ and to obtain the optimal solution $\Delta\mathbf{U}^*$, all variables of the cost function (6) have to be expressed through the optimal input trajectory $\Delta\mathbf{U}$. This can be achieved by predicting the next P outputs \mathbf{y}_k through the system dynamics (4) and (5) and by considering the input relationship $\mathbf{u}_k = \Delta\mathbf{u}_k + \mathbf{u}_{k-1}$. Then, the optimal control problem can be transformed into the linear-quadratic optimization problem

$$\Delta\mathbf{U}^* = \arg \min_{\Delta\mathbf{U}} \left\{ \frac{1}{2} \Delta\mathbf{U}^T \mathbf{H} \Delta\mathbf{U} + [\mathbf{x}_k^T \ \mathbf{Y}_d^T \ \mathbf{u}_{k-1}^T] \mathbf{F} \Delta\mathbf{U} \right\} \quad (7)$$

with the future P reference trajectory values $\mathbf{Y}_d = [\mathbf{y}_{d,k}^T \ \cdots \ \mathbf{y}_{d,k+P-1}^T]^T$, the previous input \mathbf{u}_{k-1} and the current measurement \mathbf{x}_k . The numerical solution of the optimization problem is obtained by the open-source C++ software qpOASES [2] which makes use of an online active set strategy. The state \mathbf{x}_k is non-physical and consequently can not be measured. Recapitulate that the pendulum angles and the cart positions can be measured by incremental encoders. Thus, a Kalman Filter is used to estimate the current state \mathbf{x}_k from the available measurements and the previous input variable which is needed for the optimization problem (7). Taking the first entry $\Delta\mathbf{u}_k$ of the optimal input trajectory $\Delta\mathbf{U}^*$, the control input is computed by $\mathbf{u}_k = \Delta\mathbf{u}_k + \mathbf{u}_{k-1}$. After implementing the control input \mathbf{u}_k and shifting the prediction horizon over one time step, the whole procedure is repeated with a new measurement.

Linear MPC (LMPC) relies on the accurate prediction of the future system dynamics by (4) and (5). The question arises whether the proposed scheme can cope with external disturbances or unmodeled dynamical effects. Beside these effects there is also a discrepancy between the real dynamics and the dynamics of the prediction model (4) and (5) as these equations are obtained by Jacobian linearization. In order to incorporate the mentioned uncertainties in the control design, an adaptive MPC scheme is introduced. It is the main idea of the adaptive MPC scheme, to solve an optimal control problem on the basis of a prediction of the future dynamical behaviour with a model which is updated online. Consequently, the optimization problem is adapted which leads to a consideration of parametric uncertainties and unknown disturbances in the control design and thus, to a better forecast of the future states. The following ideas are based on [11] with the main difference that these contribution deals with an adaptive control scheme of combining feedback linearization and LMPC and updating the exactly feedback linearized model. Nevertheless, all strategies have in common that a Kalman Filter is used for the online parameter adaptation of the prediction model. Therefore, the prediction model (4) and (5) is extended in order to incorporate the influence of uncertainties on the matrices \mathbf{A} and \mathbf{B} , and can be stated as

$$\mathbf{x}_{k+1} = (\mathbf{A} + \Delta\mathbf{A})\mathbf{x}_k + (\mathbf{B} + \Delta\mathbf{B})\mathbf{u}_k, \quad (8)$$

$$\mathbf{y}_k = \mathbf{C}\mathbf{x}_k + \mathbf{D}\mathbf{u}_k \quad (9)$$

with the matrices

$$\Delta \mathbf{A} = \begin{bmatrix} 0 & 0 & 0 & 0 \\ 0 & 0 & 0 & 0 \\ \theta_1 & 0 & \theta_3 & 0 \\ 0 & \theta_2 & 0 & \theta_4 \end{bmatrix}, \quad \Delta \mathbf{B} = \begin{bmatrix} 0 & 0 \\ 0 & 0 \\ \theta_5 & 0 \\ 0 & \theta_6 \end{bmatrix} \quad (10)$$

containing the unknown parameters $\boldsymbol{\theta}^T = [\theta_1 \ \cdots \ \theta_6]$. The depicted structure is chosen in that way due to the fact that in mechanical systems parameter variations usually have a direct influence on the accelerations. Parameter estimation can be transferred to state estimation by extending the state vector \mathbf{x} with the parameter vector $\boldsymbol{\theta}$ and introducing the extended state vector $\mathbf{x}_e^T = [\mathbf{x}^T \ \boldsymbol{\theta}^T]$. Assuming constant parameters $\theta_{k+1} = \theta_k$ and from (8) and (9) consequently follows the nonlinear difference equation

$$\mathbf{x}_{e,k+1} = \mathbf{f}(\mathbf{x}_{e,k}, \mathbf{u}_k) + \boldsymbol{\xi}_k, \quad (11)$$

$$\mathbf{y}_k = [\mathbf{C} \ \mathbf{0}] \mathbf{x}_{e,k} + \mathbf{D}\mathbf{u}_k + \boldsymbol{\eta}_k \quad (12)$$

with process noise $\boldsymbol{\xi}_k$ and observation noise $\boldsymbol{\eta}_k$. As the transfer behaviour in (11) from \mathbf{u} to \mathbf{y} is nonlinear, online estimation is realized by applying an UKF, see [6], in order to incorporate the nonlinearities. Unlike the Extended Kalman Filter (EKF), the UKF does not approximate the nonlinear process and thus, does not need any derivatives and is more accurate. The UKF is based on a deterministic sampling approach, where chosen sample points are propagated through the nonlinear system by an unscented transformation and capture the posterior mean and covariance accurately to the third order. A detailed description of the UKF's algorithm can be found in [6] and [14]. Recapitulate that the prediction model (8) is updated online and leads to a more accurate approximation of the dynamics. As a consequence, the quadratic programming matrices $\mathbf{H}(\boldsymbol{\theta})$, $\mathbf{F}(\boldsymbol{\theta})$ from (7) depending on the system matrices and the parameters θ_i are updated in each time step. The proposed control structure including cascade control and adaptive MPC is depicted in Figure 4.

Linear Model Predictive Control Algorithm with Disturbance Rejection

Beside the adaptation of the prediction model, uncertainties can also be considered in the control algorithm by assuming them to be external disturbances. Unlike the presented adaptive MPC, the prediction model is now kept constant. Here, the assumed external disturbances have to be estimated online in order to take corrective control actions. The algorithm is based on the discrete linear state space model

$$\mathbf{x}_{k+1} = \mathbf{A}\mathbf{x}_k + \mathbf{B}\mathbf{u}_k + \mathbf{E}\mathbf{d}_k, \quad (13)$$

$$\mathbf{y}_k = \mathbf{C}\mathbf{x}_k + \mathbf{D}\mathbf{u}_k \quad (14)$$

which is influenced by an external disturbance \mathbf{d}_k distributed onto the states by the matrix \mathbf{E} . In the same way as the other scheme, the control input is obtained by minimizing the quadratic cost function (6) over the input trajectory $\Delta \mathbf{U}$. The difference lies in the fact that the next P system outputs \mathbf{y}_k are predicted on the basis of the system dynamics (13) and (14). Consequently, the linear-quadratic optimization problem

$$\Delta \mathbf{U}^* = \arg \min_{\Delta \mathbf{U}} \left\{ \frac{1}{2} \Delta \mathbf{U}^T \mathbf{H} \Delta \mathbf{U} + [\mathbf{x}_k^T \ \mathbf{Y}_d^T \ \mathbf{u}_{k-1}^T \ \mathbf{d}_{k-1}^T] \mathbf{F} \Delta \mathbf{U} \right\} \quad (15)$$

depends on the external disturbance \mathbf{d} and thus, can take corrective action in order to minimize its influence on the tracking behaviour. The current disturbance \mathbf{d} on the system has to be estimated online, which is achieved by extending the state vector $\mathbf{x}_e^T = [\mathbf{x}^T \ \mathbf{d}^T]$. Assuming white noise on the process $\boldsymbol{\xi}_k$ and on the measurement $\boldsymbol{\eta}_k$, the linear difference equations follow

$$\mathbf{x}_{e,k+1} = [\mathbf{A} \ \mathbf{E}] \mathbf{x}_{e,k} + \mathbf{B}\mathbf{u}_k + \boldsymbol{\xi}_k, \quad (16)$$

$$\mathbf{y}_k = [\mathbf{C} \ \mathbf{0}] \mathbf{x}_{e,k} + \mathbf{D}\mathbf{u}_k + \boldsymbol{\eta}_k. \quad (17)$$

The states $\mathbf{x}_{e,k}$ and consequently the disturbances \mathbf{d}_k can be estimated online by applying a Kalman Filter. The use of an UKF is not necessarily needed as the dynamics from \mathbf{u} to \mathbf{y} is linear. It is worth to mention that the quadratic programming matrices \mathbf{H} and \mathbf{F} are constant as the system matrices are independent uncertainties.

Fuzzy-Arithmetical Uncertainty Analysis

As uncertainties in mechanical systems often result from a lack of knowledge and an inexact parameter determination, they are assumed as epistemic uncertainties and can be implemented as fuzzy numbers [5]. Fuzzy numbers can be integrated into multibody systems by fuzzy arithmetics which allows to make reliable statements concerning stability, performance, and practicability of the proposed control structures. As the dynamics of the control structure is considerably influenced by the uncertain model parameters, dealing with fuzzy numbers requires their systematic use in the dynamical analysis. A fuzzy number is defined as a convex fuzzy set with a membership function $\mu(x) \in [0 \ 1]$ only being equal to one for the

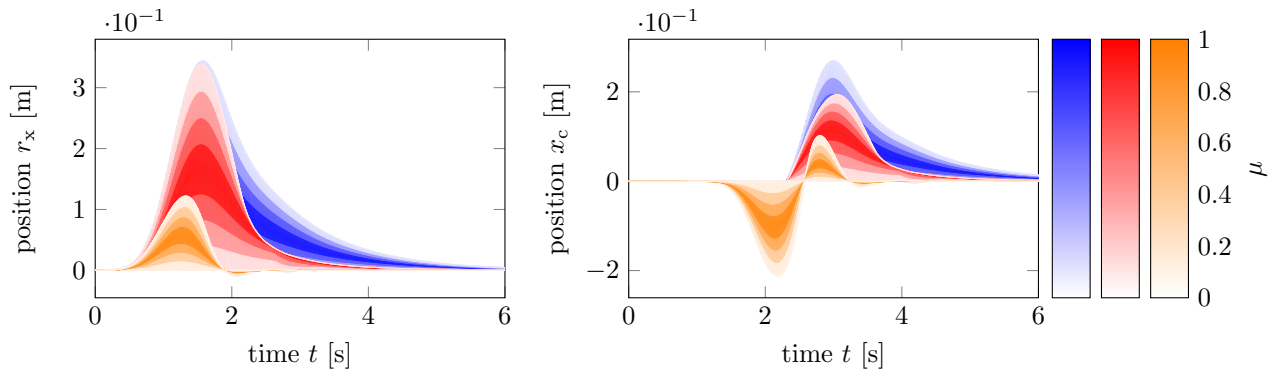


Figure 5: Fuzzy-valued sphere position r_x (left) and cart position x_c (right) of MPC ■, of adaptive MPC ■ and of MPC with disturbance rejection ■.

nominal value. In this contribution, the uncertain system parameters are described as symmetric triangular fuzzy numbers \tilde{p}_i with the membership function

$$\mu(x) = \begin{cases} 1 + (x - \hat{p}_i)/(\alpha_i \hat{p}_i), & \text{for } (1 - \alpha_i)\hat{p}_i < x \leq \hat{p}_i, \\ 1 + (x - \hat{p}_i)/(\alpha_i \hat{p}_i), & \text{for } \hat{p}_i < x < (1 + \alpha_i)\hat{p}_i, \\ 0, & \text{otherwise,} \end{cases} \quad (18)$$

where \hat{p}_i denotes the nominal value of the i -th parameter and α_i describes its deviation. A multibody simulation with fuzzy numbers \tilde{p}_i , given by their membership functions $\mu_{\tilde{p}_i}(x_i)$, can generally be described by a mapping $\tilde{q} = f(\tilde{p}_1, \dots, \tilde{p}_n)$, where \tilde{q} is for instance the fuzzy system output. The extension principle shows a way how to determine the membership function $\mu_{\tilde{q}}(y)$ of the result \tilde{q} . An efficient implementation can be realized by the transformation method [4], where the calculations are performed in terms of α -cuts. In addition, the method provides a way to quantify the effect of each fuzzy-valued parameter on the uncertainty of the system output by influence measures [3]. Providing systematic tools to analyze the influences of parameter uncertainties, the fuzzy-arithmetical analysis allows a better understanding of the dynamical behaviour of mechanical systems. It should be emphasized that the adaptivity in the control design is utilized by the UKF online, whereas the fuzzy-arithmetical analysis is only used to analyze the functionality and performance offline.

Simulative and Experimental Results

Both proposed control schemes are applied to the pendulum depicted in Figures 1 and 3. Detailed simulative and experimental investigations in the presence of two different types of uncertainties are made in order to verify the functionality of both adaptive schemes. The tuning procedure of the MPC is performed with a focus on both accurate trajectory tracking and possible application on the hardware yielding the weighting matrices $\mathbf{Q} = \text{diag}(10, 10)$ and $\mathbf{R} = \text{diag}(80, 80)$. The prediction horizon $P = 70$ is chosen quite long compared to the control horizon $M = 10$ in order to reduce the optimization problem and simultaneously to guarantee a good forecast of the dynamics, whereby the sampling time is chosen to be $\Delta t = 10$ ms. In order to make comparisons between the different schemes, all controllers have the same described tuning parameters.

First, to verify the disturbance rejection, an external disturbance $\mathbf{d} = [d \ d \ d]^T$ is assumed which represents an external force pulse acting on the center of gravity of the sphere position in x-, y- and z-direction. The disturbance value d can be described over the time t by the function

$$d(t) = \tilde{p}_1 \exp\left(\frac{-(t-1)^2}{2 \cdot 0.3^2}\right), \quad 0 \text{ s} \leq t \leq 6 \text{ s} \quad (19)$$

with its maximal value given by the triangular fuzzy number \tilde{p}_1 which is defined through its nominal value $\hat{p}_1 = 5$ N and its variation $\alpha_1 = \pm 100\%$ like in (18). In the following, adaptive MPC is referred to as the control structure with the updated model (8), whereas MPC with disturbance rejection is the control structure with disturbance estimation and rejection. The results of the MPC with the nominal model without disturbance rejection are denoted by MPC. Figure 5 displays the fuzzy-valued simulation results of the sphere position r_x and of the related cart position x_c , where the pendulum starts in its lower equilibrium position and is disturbed by the external force (19). Both fuzzy-valued results are characterized by a set of possible solutions, where the membership values μ are indicated by their coloring. The nominal solution is given by the membership value $\mu = 1$ and is represented by the strongest colour. It can be seen that the external disturbance has a great impact on the sphere position which is deflected from its equilibrium up to 30 cm. The results demonstrate a significant difference in the disturbance rejection between the MPC schemes. It is obvious that the non-adaptive MPC has the worst rejection behaviour which can be significantly improved by the adaptive MPC reacting to the external disturbance by changing its prediction model. The MPC with disturbance rejection has by far the

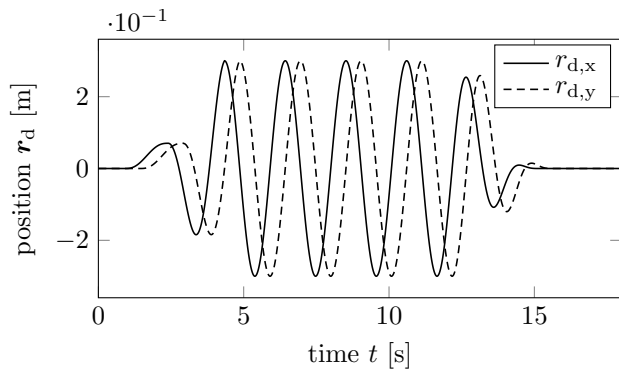


Figure 6: Circular reference trajectory r_d for the sphere position.



Figure 7: Sphere of the pendulum with an additional mass connected to the sphere by a spring.

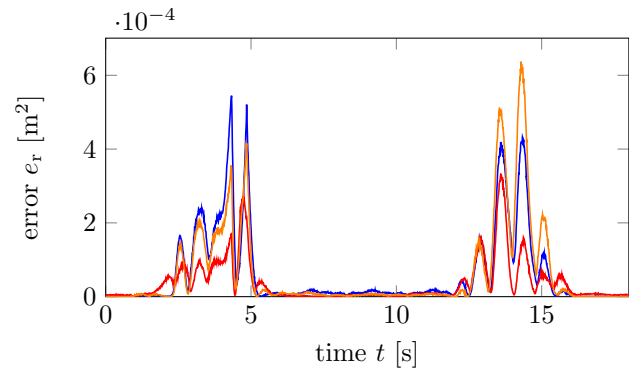
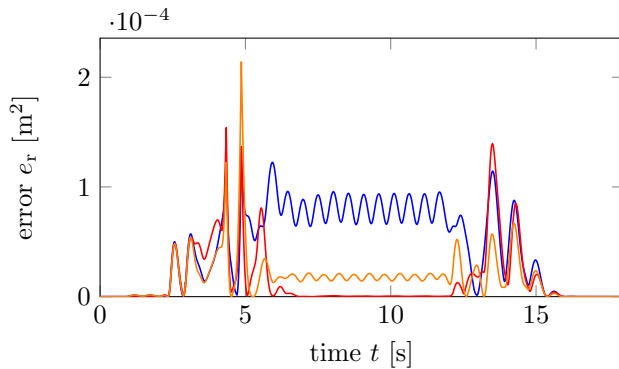


Figure 8: Simulative (left) and experimental (right) quadratic tracking error $e_r = \|r_d - r\|_2^2$ of MPC — , of adaptive MPC — , and of MPC with disturbance rejection — .

best rejection behaviour. This is caused by the fact that the value of the external pulse is estimated online and is taken into account by the optimization problem (15). As a consequence, the carts act earlier and more appropriate leading to a satisfying suppression which is shown by both plots of Figure 5.

Furthermore, the tracking behaviour in the presence of uncertainties is investigated. The reference trajectory r_d for the sphere position consists of a circular motion with an amplitude of 30 cm which is depicted in Figure 6. As the average calculation times of all three algorithms for one time step are smaller than the chosen sample time $\Delta t = 10$ ms, simulative and experimental investigations can be made. To verify the tracking capability of all control schemes, both simulative and experimental quadratic tracking errors e_r are depicted in Figure 8 under the assumption of no additional disturbances. Both plots approve the functionality of all schemes both for simulation and hardware. Nevertheless, especially the simulation results show that the tracking error is strongly reduced by those MPC schemes considering uncertainties in their algorithm. The reason for this is that due to Jacobian linearization there is a discrepancy between the real dynamics and the dynamics of the prediction model for the MPC. The adaptive MPC closes this discrepancy by an adaptation of its dynamics, whereas the MPC with disturbance rejection considers this discrepancy as an external disturbance. In order to demonstrate the effect of unmodeled dynamics on the control schemes, the pendulum is disturbed with an additional mass which is connected to the sphere by a spring, see Figure 7. The pendulum can now be seen as a double pendulum with three additional degrees of freedom as the spring is universal-mounted to the bottom of the sphere. Note that the weight of the additional mass $m_a = 1$ kg is relatively high compared to the mass of the sphere and the rod $m_{res} = m_s + m_r = 5.15$ kg and, thus, significantly influences the dynamics of the pendulum. In order to quantify the influence, the additional mass m_a is implemented as a triangular fuzzy number \tilde{p}_2 which is defined through its nominal value $\hat{p}_2 = 1$ kg and its variation $\alpha_2 = \pm 100\%$. Figure 9 depicts the simulation results of the fuzzy-valued quadratic tracking error. It can be seen that all three controllers can cope with the additional unknown dynamics, whereas both adaptive MPC and MPC with disturbance rejection further reduce the tracking error. As the adaptive MPC has the capability to adapt its dynamics to the new environment online, it becomes clear that it shows best tracking behaviour which is also confirmed by Figure 8. The simulation results are verified by the experimental results shown in Figure 10. As it can be seen from the left plot, the amplitude of the sphere position of 30 cm can only be sufficiently tracked with the use of the adaptive schemes, whereas the nominal MPC scheme exhibits a remaining offset. This is caused by the fact that, in case of adaptive schemes, the amplitudes of the cart position x_c are slightly larger than in the nominal case which drives the sphere position to the exact trajectory. The unknown model parameters θ_i of the adaptive MPC are exemplarily shown in order to demonstrate that these parameters vary over the time. Although the parameters have no physical meaning, one can follow that parts of the disturbed dynamics are correctly represented by the prediction model (4) as the parameters θ_1 and θ_2 remain zero.

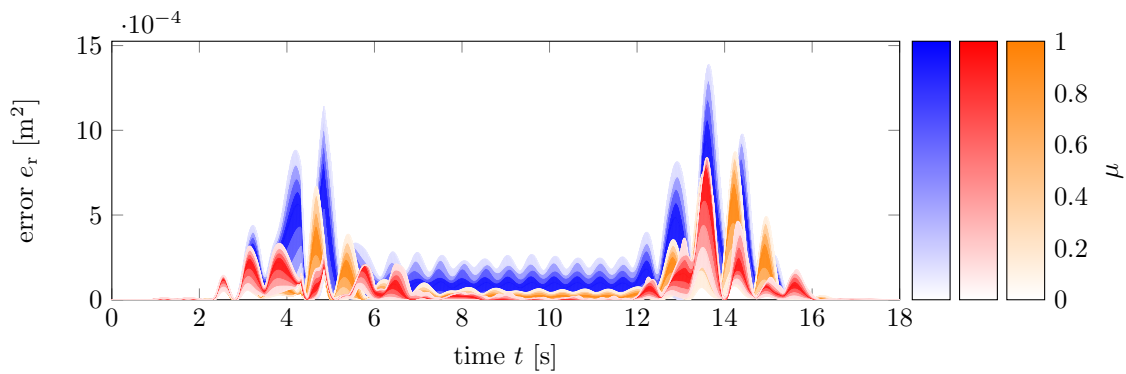


Figure 9: Fuzzy-valued quadratic tracking error $e_r = \|\mathbf{r}_d - \mathbf{r}\|_2^2$ of MPC ■, of adaptive MPC ■ and of MPC with disturbance rejection ■.

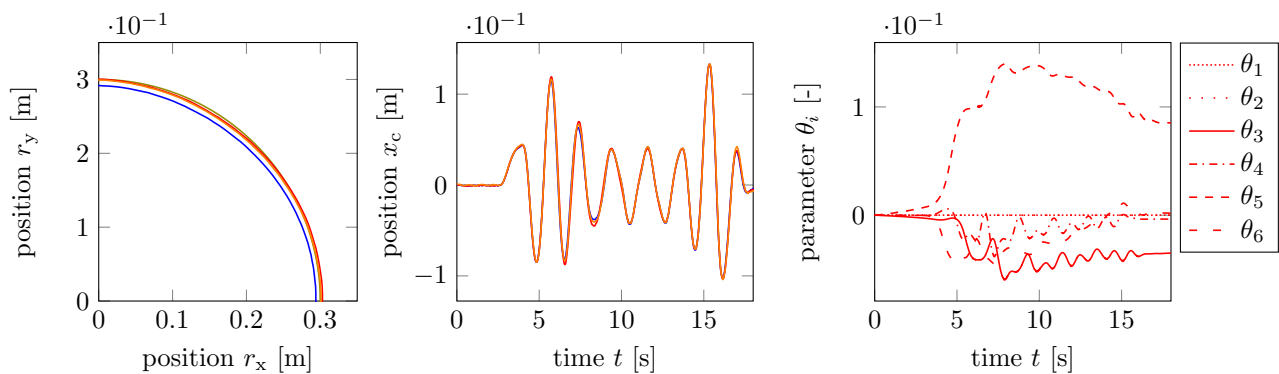


Figure 10: Experimental results of pendulum with additional mass: sphere position \mathbf{r} (left), cart position x_c (middle), and estimated model parameters θ_i (right) of MPC —, of adaptive MPC —, and of MPC with disturbance rejection —.

Conclusions

The simulative and experimental application of an adaptive MPC scheme for a three-dimensional pendulum has been presented. A cascade control structure is chosen consisting of a fast position control and an adaptive MPC in order to cope with uncertainties in the motors. The adaptive MPC is based on an online-adaptation of the prediction model which is realized by an UKF. Fuzzy-arithmetical simulation results and experimental data have demonstrated an improvement with the adaptive MPC compared to the nominal MPC both in disturbance rejection and trajectory tracking in the presence of different uncertainties. As the nominal MPC also leads to acceptable results, the choice between the nominal and the adaptive MPC depends on the control objective and the type and value of the uncertainty.

References

- [1] K. J. Astrom. Theory and applications of adaptive control - a survey. *Automatica*, 19(5):471–486, 1983.
- [2] H. Ferreau, C. Kirches, A. Potschka, H. Bock, and M. Diehl. qpOASES: A parametric active-set algorithm for quadratic programming. *Mathematical Programming Computation*, 6(4):327–363, 2014.
- [3] U. Gauger, S. Turrin, M. Hanss, and L. Gaul. A new uncertainty analysis for the transformation method. *Fuzzy Sets and Systems*, 159:1273–1291, 2008.
- [4] M. Hanss. The transformation method for the simulation and analysis of systems with uncertain parameters. *Fuzzy Sets and Systems*, 130:277–289, 2002.
- [5] M. Hanss. *Applied Fuzzy Arithmetic – An Introduction with Engineering Applications*. Springer, Berlin, 2005.
- [6] S. J. Julier and J. K. Uhlmann. New extension of the Kalman filter to nonlinear systems. In *AeroSense'97*, pages 182–193. International Society for Optics and Photonics, 1997.
- [7] M. Morari and J. H. Lee. Model predictive control: Past, present and future. *Computers & Chemical Engineering*, 23(4):667–682, 1999.
- [8] S. J. Qin and T. A. Badgwell. A survey of industrial model predictive control technology. *Control Engineering Practice*, 11(7):733–764, 2003.
- [9] H. Sage, M. De Mathelin, and E. Ostertag. Robust control of robot manipulators: a survey. *International Journal of Control*, 72(16):1498–1522, 1999.
- [10] F. Schnelle and P. Eberhard. Real-time model predictive control of a pendulum. *PAMM*, 14(1):907–908, 2014.
- [11] F. Schnelle and P. Eberhard. Adaptive nonlinear model predictive control design of a flexible-link manipulator with uncertain parameters. *Acta Mechanica Sinica*, DOI:10.1007/s10409-017-0669-4, 2017.
- [12] R. Seifried, T. Gorius, and P. Eberhard. Control design for the interactive 3D-pendulum presented at the world exhibition EXPO 2010. *Journal of System Design and Dynamics*, 5:937–952, 2011.
- [13] J.-J. E. Slotine and W. Li. On the adaptive control of robot manipulators. *The International Journal of Robotics Research*, 6(3):49–59, 1987.
- [14] E. Wan and R. van der Merwe. The unscented Kalman filter for nonlinear estimation. In *Adaptive Systems for Signal Processing, Communications, and Control Symposium 2000*, pages 153–158, 2000.